HHS Public Access

Author manuscript

Nat Med. Author manuscript; available in PMC 2014 May 01.

Published in final edited form as:

Nat Med. 2013 November ; 19(11): 1489–1495. doi:10.1038/nm.3368.

Cold-inducible RNA-binding protein (CIRP) triggers inflammatory responses in hemorrhagic shock and sepsis

Xiaoling Qiang[#1], **Weng-Lang Yang**[#1], **Rongqian Wu**[1], **Mian Zhou**[1], **Asha Jacob**[1], **Weifeng Dong**[1], **Michael Kuncewitch**[1], **Youxin Ji**[1], **Huan Yang**[2], **Haichao Wang**[2], **Jun Fujita**[3], **Jeffrey Nicastro**[1], **Gene F. Coppa**[1], **Kevin J. Tracey**[2], and **Ping Wang**[1]

[1]Center for Translational Research, The Feinstein Institute for Medical Research, Manhasset, New York, USA.

[2]Center for Biomedical Science, The Feinstein Institute for Medical Research, Manhasset, New York, USA.

[3]Department of Clinical Molecular Biology, Kyoto University, Kyoto, Japan.

[#] These authors contributed equally to this work.

Abstract

Excessive production of proinflammatory mediators is observed in patients undergoing hemorrhagic and septic shock. Here, we report the detection of cold-inducible RNA-binding protein (CIRP) in the blood of surgical ICU individuals. In animal models of hemorrhage and sepsis, CIRP is up-regulated in several organs and released into the circulation. Under hypoxic stresses, CIRP in macrophages is translocated from the nucleus to the cytosol and actively released. Recombinant CIRP stimulates TNF-α and HMGB1 release in macrophages as well as induces inflammatory responses and causes tissue injury in animals. Antisera to CIRP attenuate shock-induced inflammation, tissue injury, and lethality. Extracellular CIRP's activity is mediated through the TLR4/MD2 complex. Surface plasmon resonance analysis indicates that CIRP binds to the TLR4/MD2 complex as well as to individual TLR4 and MD2. The human CIRP amino-acid segment 106-125 binds to MD2 with high affinity. Collectively, CIRP is a new proinflammatory mediator of shock.

Please address correspondence, proofs, and reprint requests to: Ping Wang, M.D. Center for Translational Research The Feinstein Institute for Medical Research 350 Community Drive Manhasset, NY 11030, USA Tel: (516) 562-3411 Fax: (516) 562-2396 pwang@nshs.edu.

AUTHOR CONTRIBUTIONS

X.Q. and M.Z. performed the experiments and analyzed data. W.-L.Y. conducted the translocation study, designed and coordinated SPR analysis, and wrote the manuscript. R.W. designed the experiments. A.J. assisted with the design of experiments and participated in manuscript editing. W.D. and Y.J. performed animal studies. M.K. collected the serum from surgical ICU patients and analyzed human data. J.N. and G.F.C. analyzed animal studies. H.Y. and K.J.T. assisted in the knockout mice study and SPR analysis. F.J. assisted in the CIRP knockout mice and GFP-CIRP study and revised the manuscript. H.W. assisted with the design of the study and analyzed data. P.W. designed and supervised the study and revised the manuscript.

COMPETING FINANCIAL INTERESTS

One of the authors (P.W.) is an inventor of the pending PCT application #WO/2010/120726: “Treatment of inflammatory diseases by the inhibition of cold shock proteins.” This patent application covers the fundamental concept of using CIRP inhibitors for the treatments of inflammatory diseases. Other authors declare no competing financial interests.

INTRODUCTION

Traumatic injury brings 37 million people to emergency rooms each year and is a leading cause of death in the US[1]. Hemorrhagic shock from loss of blood volume is a major cause of morbidity and mortality following trauma[2]. During fluid resuscitation, excessive amounts of inflammatory cytokines are produced, causing systemic inflammatory response syndrome (SIRS) and multiple organ dysfunction[3]. Sepsis is another clinical condition associated with SIRS and often happens in the ICU, with an overall mortality of 30% in the US[4]. Sepsis is originally defined as severe systemic inflammation occurred in the host in response to invading pathogens[5].

Systemic inflammation can be triggered by exogenous pathogen-associated molecular pattern molecules (PAMPs) expressed on invading microorganisms during infection or by endogenous damaged-associated molecular pattern molecules (DAMPs) released from host cells during tissue injury[6,7]. Both PAMPs and endogenous DAMPs are recognized by immune cells through a group of pattern-recognition receptors (PRRs), including Toll-like receptors (TLRs), receptor of advanced glycation end products (RAGEs), C-type lectin receptors, scavenger receptors, and complement receptors[8-10]. After engaging with the receptors, several signaling pathways are activated, leading to the production of various inflammatory mediators including cytokines, chemokines, and vasoactive peptides[6,11,12]. While the involvement of microbial PAMPs is bolstered by long-standing evidence, the concept of the role of endogenous molecules in inducing inflammation has just begun to emerge. In recent years, several molecules varying in both structure and intracellular function have been identified as alarmin danger signals in triggering immune responses. Members of this growing alarmin family include HMGB1 (ref.[13,14]), heat shock proteins[15], uric acid[16], S100 proteins[17], histones[18], and mitochondrial DNA[19].

CIRP is from the family of cold shock proteins that respond to cold stresses. Murine and human CIRP is a 172-aa (95% identical) nuclear protein consisting of one amino-terminal consensus sequence RNA-binding domain and one carboxyl-terminal glycine-rich domain, and functions as an RNA chaperone to facilitate translation (**Supplementary Fig. 1**)[20-22]. CIRP is constitutively expressed at low levels in various tissues[20,23,24], becoming up-regulated during mild hypothermia[22] as well as exposure to UV irradiation[25] and hypoxia[26]. Here, we revealed that extracellular CIRP was an endogenous proinflammatory mediator causing deleterious effects during hemorrhagic and septic shock. Thus, CIRP antagonism might serve as a previously unappreciated therapeutic strategy.

RESULTS

CIRP is increased in hemorrhaged humans and animals

To explore the role of CIRP in clinical conditions, we examined the serum CIRP levels from ten surgical ICU individuals (**Supplementary Table 1**). There were five females and five males and the average age was 71 years old. The Acute Physiology and Chronic Health Evaluation II (APACHE II) ranged from 13 to 25 and averaged 19. The average blood sample collection time was 43 h after the onset of shock, which was defined by a clinically documented systolic blood pressure < 90 mmHg either during active hemorrhage or

following a traumatic insult. Serum CIRP was well detected in all ten individuals regardless of differences in clinical parameters, while being hardly observed in healthy volunteers (**Fig. 1a**).

We then performed a rat model of hemorrhagic shock by bleeding the animals to a mean arterial pressure (MAP) of 25–30 mmHg and maintaining that MAP for 90 min, followed by fluid resuscitation. Serum CIRP was detectable at 240 min and was found to be significantly elevated at 330 min post-shock in hemorrhaged rats (**Fig. 1b**). CIRP protein levels started to increase at 150 and 240 min in the liver and heart, respectively (**Fig. 1b**). Correspondingly, CIRP mRNA levels were significantly induced in the liver and heart at 240 min post-shock by 4.1 and 2.8-fold, respectively (**Fig. 1c**).

CIRP is released from macrophages exposed to hypoxia

Since CIRP was detectable in the serum of both humans and rats after shock, we planned to determine the mode of CIRP release. Macrophages are the major cell population responsible for the release of various inflammatory mediators. We subjected murine macrophage-like RAW 264.7 cells to hypoxia in the similar manner in which it occurs during hemorrhagic shock, and examined the cellular location of CIRP. CIRP was primarily located in the nucleus during normoxic conditions, whereas cytoplasmic CIRP was detected at 7 h and markedly increased at 24 h after reoxygenation from 20-h hypoxia determined by biochemical fractionation (**Fig. 1d**). We also used a genetic approach to confirm the translocation of CIRP. In a control experiment in which RAW 264.7 cells were transfected with a green fluorescence protein (GFP) expression plasmid, green fluorescence was observed all over the cell in both normoxic and hypoxic conditions **(Supplementary Fig. 2**). In contrast, when RAW 264.7 cells were transfected with a GFP-CIRP expression plasmid, green fluorescence was only observed in the center of the cell, while being overlapped by blue fluorescence from Hoechst nuclei staining under normoxia (**Fig. 1e**). However, at 4 h after reoxygenation from hypoxia, green fluorescence was distributed throughout both the nucleus and cytoplasm (**Fig. 1e**). Taken together, hypoxia followed by reoxygenation induced CIRP translocation from the nucleus to the cytoplasm in macrophages.

We then examined the possibility whether cytoplasmic CIRP could be released into the extracellular space. In the conditioned medium of RAW 264.7 cells, CIRP was well detected at 24 h reoxygenation after hypoxia, while it was undetectable in normoxia by Western blotting (**Fig. 1f**). Furthermore, the intracellular CIRP protein level increased by 2.8-fold immediately after hypoxia and 4.3-fold after 7 h of reoxygenation, while its level was reduced at 24 h of reoxygenation due to its release into the extracellular space (**Fig. 1f,g**). CIRP release was not attributed to necrosis since there was no change in lactate dehydrogenase activity and no detectable intracellular Bax protein in the conditioned medium after hypoxia (data not shown).

The CIRP protein sequence does not contain a secretion leader signal; therefore, its secretion should not be through the classical (endoplasmic reticulum-Golgi-dependent) pathway[27]. To identify a potential mechanism of active CIRP release, we conducted a biochemical fractionation to isolate the lysosomal compartment of RAW 264.7 cells undergoing hypoxia.

During normoxia, CIRP protein was not detected in lysosomes, while it was co-localized with cathespin D, a protein maker of lysosomes, at 24 h reoxygenation form hypoxia (**Fig. 1h**). This result indicated that CIRP could be released by the lysosomal secretion.

Recombinant CIRP induces inflammatory responses

To address whether the extracellular CIRP could function as an inflammatory mediator, we expressed and purified recombinant murine CIRP (rmCIRP) using a bacterial expression system with more than 97% purity and confirmation by Western blotting (**Supplementary Fig. 3a,b**). We had conducted a Triton X-114 extraction procedure to remove lipopolysaccharide (LPS)[28] from purified rmCIRP with residual ~10 pg LPS/μg CIRP measured by the Limulus amebocyte lysate assay, which was comparable to that described in other identified endogenous DAMPs[29,30]. Addition of rmCIRP to RAW 264.7 cells increased TNF-α release in a dose- and time-dependent manner (**Fig. 2a,b**). rmCIRP also dose-dependently induced the release of another proinflammatory cytokine, HMGB1 (**Fig. 2c**). In addition to the *in vitro* effect, administration of rmCIRP to healthy rats significantly increased serum TNF-α, IL-6, and HMGB1 levels as well as the organ injury markers aspartate aminotransferase (AST) and alanine aminotransferase (ALT) (**Supplementary Fig. 4**).

To exclude the concern of LPS residue in rmCIRP being responsible for cytokine release, we demonstrated that polymyxin B, an LPS-binding antibiotic, did not interfere with rmCIRP-induced TNF-α production, while heat treatment inactivated rmCIRP's activity (**Fig. 2d**). In contrast, polymyxin B inhibited LPS-induced TNF-α release by 84%, while heat treatment only slightly lowered LPS's activation (**Fig. 2d**). To further avoid the LPS contamination in the preparation of recombinant proteins, we obtained recombinant human CIRP (rhCIRP) expressed and purified from human HEK293 cells. rhCIRP had comparable activity to rmCIRP in stimulating TNF-α release from differentiated human THP-1 cells (**Fig. 2e**) as well as primary human peripheral blood mononuclear cell (PBMC) in a dose-dependent manner (**Fig. 2f**). Thus, stimulation of cytokine release by CIRP was not attributable to LPS contamination. Furthermore, CIRP-induced cytokine activation was conserved between rodents and humans.

It has been reported that HMGB1 can also stimulate TNF-α release[31]. We then analyzed the relationship between CIRP and HMGB1 on stimulating TNF-α release by applying respective neutralizing antisera. We generated antisera to CIRP that effectively inhibited TNF-α production by rmCIRP in RAW 264.7 cells in a dose-dependent manner (**Supplementary Fig. 3c,d**). Pre-incubation with antisera to HMGB1(ref. [32]) resulted in a 31% reduction of the TNF-α release induced by rmCIRP in THP-1 cells without statistical significance, while pre-incubation with antisera to CIRP had a significant 70% reduction (**Fig. 2g**). Vice versa, pre-incubation with antisera to CIRP only resulted in a 17% reduction of TNF-α release induced by rmHMGB1 without statistical significance (**Fig. 2g**). Furthermore, rmCIRP, rmHMGB1, and rmCIRP plus rmHMGB1 induced TNF-α levels of 0.8, 0.6, and 1.6 ng/ml, respectively (**Fig. 2g**). Taken together, these results indicated that CIRP and HMGB1 worked additively in stimulating TNF-α release from macrophages.

Neutralization of CIRP attenuates hemorrhage and sepsis

We first determined whether extracellular CIRP played a role in mediating inflammatory responses during hemorrhage. Administration of neutralizing antisera to CIRP to hemorrhaged rats significantly reduced serum and hepatic levels of TNF-α and IL-6, which remained unaltered by non-immunized control IgG (**Fig. 3a**). Serum AST and ALT, as well as liver myeloperoxidase activity - indicative of neutrophil accumulation - were significantly reduced in the antisera to CIRP group (**Fig. 3b**). Finally, the survival rate of the antisera to CIRP group was significantly higher than that of the control IgG and vehicle groups ten days after hemorrhage (85% *vs*. 38% and 43%; **Fig. 3c**). Concordantly, the survival rate of *Cirp*$^{-/-}$ mice was significantly higher than that of wild-type mice 72 h after hemorrhage (56% *vs*. 11%; **Fig. 3d**). We also observed a 7.3-fold increase of serum TNF-α in wild-type mice at 4 h after hemorrhage; such TNF-α elevation did not occur in *Cirp*$^{-/-}$ mice (**Fig. 3e**). A similar phenomenon was observed in serum HMGB1 levels (**Fig. 3f**), suggesting that CIRP and HMGB1 both acted in contributing to the mortality of animals after shock.

We then extended the study of CIRP's pro-inflammatory activity to sepsis, another clinical condition caused by hyperinflammation. We examined the CIRP expression in rats subjected to cecal ligation and puncture (CLP), an established animal model of polymicrobial sepsis[33]. At 20 h after CLP, serum levels of CIRP were increased by 3.4-fold, compared to the sham (**Fig. 4a**). Similarly, mRNA and protein levels of CIRP in the liver were also increased by 2.4- and 4.0-fold, respectively (**Fig. 4b,c**). We further assessed the effect of LPS on regulating CIRP expression and release in macrophages. The mRNA and protein levels of CIRP in rat primary peritoneal macrophages were markedly increased after exposure to LPS for 6 and 24 h, respectively (**Fig. 4d,e**). CIRP protein was also detected in the conditioned medium after 6-h exposure to LPS, while it was undetectable from non-treated cells (**Fig. 4e**). We then explored the possibility of other inflammatory mediators inducing CIRP release. Incubation of RAW 264.7 cells with rmHMGB1 and rmTNF-α for 24 h did not cause CIRP release into the medium, whereas CIRP protein was detectable from cells exposed to LPS (**Fig. 4f**). To validate the detrimental activity of extracellular CIRP, we administered neutralizing antisera to CIRP to septic animals. The ten-day survival rate of septic rats significantly increased from 39% to 78% after treatment with antisera to CIRP (**Fig. 4g**). Thus, CIRP also served as a detrimental factor in septic shock.

CIRP induces inflammatory responses through TLR4

We further determined the cell surface receptors responsible for transmitting extracellular CIRP signaling. Three major PRRs known to mediate inflammation were examined: RAGE, TLR2, and TLR4 (ref. [8-10]). By comparing the difference among wild-type and knockout mice targeting each receptor in response to rmCIRP, we found that only TLR4-difficient macrophages lost the response for TNF-α induction, while RAGE- and TLR2-deficient macrophages maintained similar responses to wild-type macrophages (**Fig. 5a**). To confirm the requirement of TLR4 in mediating CIRP activity, we injected rmCIRP to wild-type and *Tlr4*$^{-/-}$ mice. Similar to rats, wild-type mice exhibited an increase of serum proinflammatory cytokines (TNF-α, IL-6, and HMGB1) and organ injury markers (AST and ALT) in a dose-dependent manner to rmCIRP injection (**Fig. 5b,c**). In contrast, these deleterious effects of rmCIRP on the wild-type mice were diminished in *Tlr4*$^{-/-}$ mice (**Fig. 5b,c**).

We then applied surface plasmon resonance (SPR) analysis to determine the physical interaction between CIRP and the receptors. TLR4 often accompanies MD2, as a co-receptor, to form the TLR4/MD2 complex[34]. All the recombinant proteins were derived from human coding sequence for SPR analysis. rhCIRP bound to rhTLR4, rhMD2, and the rhTLR4/MD2 complex with an apparent K_D of 6.17×10^{-7}, 3.02×10^{-7}, and 2.39×10^{-7} M, respectively (**Table 1** and **Supplementary Fig. 5**). We also examined the binding of rhMD2 to rhTLR4 as a positive control and obtained an apparent K_D of 5.37×10^{-8} M, which is very close to the K_D of 6.29×10^{-8} M, as previously reported by a recent study[35]. Notably, rhCIRP had a K_D in the nM range with RAGE and TLR2 (**Table 1** and **Supplementary Fig. 5**); however, the biological significance of these bindings remains to be determined. These SPR results clearly indicated that CIRP was capable of interacting with different types of proteins, which fits its character as a chaperone protein. We further determined the region of CIRP that bound to MD2. We synthesized 32 oligopeptides (15-mer) covering the entire human CIRP sequence and performed a series of SPR analyses. Three oligopeptides, aa 101-115, 106-120, and 111-125 bound to rhMD2 with high affinity (**Fig. 5d** and **Supplementary Fig. 6**).

DISCUSSION

Current understanding of the biological function of intracellular CIRP is that it functions to stabilize specific mRNAs and facilitate translation for survival advantage when cells are under stress conditions[36,37]. In this study, we provide several lines of evidence to support the discovery that extracellular CIRP is a new DAMP. Firstly, CIRP is detected in the serum of surgical ICU individuals as well as hemorrhaged and septic animals. Secondly, CIRP is translocated from the nucleus to the cytoplasm and actively released from macrophages under the hypoxic stress or exposure to LPS. Thirdly, recombinant CIRP proteins induce TNF-α release from macrophages *in vitro,* stimulate inflammatory responses and cause tissue injury in animals. Fourthly, the inhibition of extracellular CIRP activity by neutralizing antisera to CIRP significantly improves the survival of hemorrhaged and septic animals. Finally, CIRP interacts with TLR4, which is one of the PRRs that is commonly utilized by DAMPs to trigger inflammatory responses. Thus, extracellular CIRP is a *bona fide* proinflammatory mediator.

We have demonstrated that CIRP is translocated from the nucleus to the cytoplasm in RAW 264.7 cells after exposure to hypoxia. Such CIRP translocation has also been observed in other cell types, including fibroblasts and epithelial cells, when under UV exposure, osmotic shock, heat shock and endoplasmic reticulum stresses[38,39]. Methylation of arginine residues in the RGG domain under environmental stresses[38] and phosphorylation at the C-terminal region in response to UV radiation[39] have been postulated for regulating CIRP exit from the nucleus. We also observed the release of CIRP into the conditioned medium in response to hypoxia or LPS. A number of non-canonical pathways have been proposed for release of "leaderless" proteins, including microvesicle shedding, exocytosis of secretory lysosomes, and active transport[27]. In addition, an alternative model of leaderless IL-1β secretion can be completed by formation of multivesicular bodies containing exosomes with entrapped IL-1β and later fusion of these multivesicular bodies with the plasma membrane to release exosomes[40]. In this study, we have demonstrated that CIRP can be released through the

lysosomal secretion; whether other mechanisms are utilized for CIRP release needs further investigation.

Identification of CIRP's TLR4-mediated proinflammatory activity is consistent with previous studies showing that TLR4 plays a significant role in mediating inflammation and organ injury in hemorrhaged animals[41] as well as septic animals[42]. TLR4 can also recognize several endogenous molecules, including HMGB1, heat shock proteins, hyaluronic acid, and fibronectin when they are released from stressed, damaged or dying cells, or from degradation of the extracellular matrix[43-46]. Although many DAMPs serve as ligands of the TLR4/MD2 complex, some molecules may bind to the different sites of the TLR4/MD2 complex and work additively in stimulating proinflammatory cytokine production in macrophages, as we have demonstrated here via the relationship between CIRP and HMGB1. As indicated by SPR analysis, HMGB1 binds to the TLR4/MD2 complex with a K_D of 1.5×10^{-6} M[47], which is comparable to CIRP's ($K_D = 2.39 \times 10^{-7}$ M). Further analysis indicates that HMGB1 binds to MD2 with a K_D of 8×10^{-9} M, but does not bind to TLR4 (ref. [48]), whereas we show that CIRP can bind to individual MD2 and TLR4. Mapping the subdomains of CIRP that interact with TLR4, MD2 and the TLR4/MD2 complex is our ongoing investigation as we seek to obtain more information on the overall molecular structure of CIRP as it concerns in binding to these receptors. Of note, the K_D of LPS to TLR4 and MD2 is 1.41×10^{-5} and 2.33×10^{-6} M, respectively[49].

Discovery of CIRP as a new inflammatory mediator not only advances our understanding of an alternative mechanism in inducing inflammation, but also helps in the development of new therapeutic strategies. We have already demonstrated that CIRP can be actively released, despite the fact that “leaderless” proteins can be leaked out by passive modes, such as necrosis[50]. In support of our findings, a recent study reports the involvement of CIRP in activating the NF-κB pathway for regulating IL-1β expression in cultured fibroblasts[51]. In this study, we have developed neutralizing antisera to CIRP as treatment and demonstrated their efficacy in improving the survival of hemorrhaged and septic animals. Thus, targeting CIRP may provide therapeutic potential to ameliorate morbidity and mortality for victims of hemorrhage and sepsis.

ONLINE METHODS

Human blood specimens

Blood samples were obtained from patients admitted to the surgical intense care unit (ICU). Serum was separated and stored in aliquots at –80 °C. Informed consent and human subject protocols were approved by the Institutional Review Board (IRB) of the North Shore-Long Island Jewish Health System.

Experimental animals

Male Sprague-Dawley rats (Charles River, Wilmington, Massachusetts), weighing 275 to 325 g, were used in the experiments. *Cirp*$^{-/-}$ mice with C57BL/6 background were provided by Kumamoto University, Japan[52]. *Rage*$^{-/-}$, *Tlr2*$^{-/-}$, and *Tlr4*$^{-/-}$ mice as described in the previous study were maintained at the Feinstein Institute for Medical Research[47]. C57BL/6

wild-type mice were purchased from Jackson Laboratory (Bar Harbor, Maine). Male and age-matched (10 to 12 weeks) mice were used in the experiments. Animals were randomly assigned to the sham, vehicle control, or treatment groups. The number of animals used in each group was based on our previous publications on animal models of hemorrhage and sepsis. All animal studies were not conducted in a completely blinded fashion. Animals were excluded from the analysis if they died during the surgical operation. All experiments were performed in accordance with the guidelines for the use of experimental animals by US National Institutes of Health (Bethesda, Maryland) and were approved by the Institutional Animal Care and Use Committee (IACUC) at the Feinstein Institute for Medical Research.

Animal model of hemorrhagic shock

Animals were anesthetized with isoflurane inhalation. Catheters (PE-50 tubing) were placed in both femoral veins and arteries. The animal was bled to a mean arterial pressure of 25–30 mmHg within 10 min. This pressure was maintained for 90 min and then animals were resuscitated with lactated Ringer's solution (the equivalent of two times the maximum bleed-out volume) over a 60-min period. Sham-operated animals underwent the same surgical procedure without bleeding and resuscitation.

Animal model of polymicrobial sepsis

Animals were anesthetized with isoflurane inhalation. Cecal ligation and puncture (CLP) was performed through a midline laparotomy. Briefly, a 2-cm midline abdominal incision was performed. The cecum was exposed, ligated just distal to the ileocecal valve to avoid intestinal obstruction, punctured twice with an 18-gauge needle, squeezed slightly to allow a small amount of fecal matter to flow from the holes, and then returned to the abdominal cavity. The abdomen was closed in layers with suture. Sham-operated animals underwent the same procedure with the exception that the cecum was neither ligated nor punctured. The animals were resuscitated with 3 ml per 100 g body weight normal saline subcutaneously immediately after surgery.

Cell culture and isolation of peritoneal macrophages

Murine macrophage-like RAW 264.7 cells and human monocyte THP-1 cells were obtained from ATCC (Manassas, Virginia). Primary peritoneal macrophages were isolated from C57BL/6 wild-type, *Rage*$^{-/-}$, *Tlr2*$^{-/-}$, and *Tlr4*$^{-/-}$ mice at day three after intraperitoneal injection with 4% thioglycolate as described earlier[47]. Rat primary peritoneal macrophages were directly isolated from the abdominal cavity of a male Sprague-Dawley rat without pre-induction. RAW 264.7 cells and peritoneal macrophages were cultured in DMEM and RPMI1640 (Invitrogen, Grand Island, New York), respectively. THP-1 cells were cultured in RPMI1640 with 0.05 mM β-mercaptoethanol and differentiated into macrophage-like cells by incubating with phorbol 12-myristate 13-acetate (20 ng m^{-1}) for 48 h. All cultured media were supplemented with 10% heat-inactivated FBS, 1% penicillin/streptomycin and 2 mM glutamine. Cells were maintained in a 37 °C incubator with 5% CO_2.

Isolation of human PBMC

Human PBMCs were isolated from blood obtained from healthy donors at the New York Blood Bank by centrifugation over a Ficoll-Paque Plus (GE Healthcare, Port Washington, New York) density gradient according to standard protocols. Isolated cells were washed with RPMI1640 complete medium and cultured on a plate. After 2 h, the non-adherent cells were removed and attached cells were cultured overnight before use.

Administration of rmCIRP and antisera to CIRP

One ml of rmCIRP or normal saline (vehicle) was administered intravenously to healthy animals. Antisera to CIRP, rabbit control IgG, or vehicles were administered to hemorrhaged rats 15 min after the initiation of fluid resuscitation over a period of 45 min via the femoral venous catheter.

Survival study

The hemorrhaged rats were administered antisera to CIRP, rabbit control IgG, or normal saline (vehicle) for three consecutive days and their mortalities were monitored for ten days. Wild-type and *Cirp*$^{-/-}$ mice were subjected to hemorrhage and survival was recorded for 72 h. The septic rats were administered antisera to CIRP or rabbit control IgG at 5 h after CLP. Necrotic cecum was removed 20 h after CLP and their mortalities were monitored for ten days.

RT-PCR assay

Total RNAs were extracted by Trizol (Invitrogen). The cDNA was synthesized using MLV reverse transcriptase (Applied Biosystems, Grand Island, New York). PCR reaction was performed in QuantiTect SYBR Green PCR mixture (Qiagen, Valencia, California), and analyzed by the Applied Biosystems 7300 PCR System. GAPDH was used as an internal control for normalization and the relative expression level of the analyzed gene was calculated by the $\Delta\Delta Ct$-method. Each sample was measured in duplicates. The RT-PCR primers were synthesized from Operon (Huntsville, Alabama). The primer sequences are listed as following: rat CIRP (NM_031147), 5'-GGG TCC TAC AGA GAC AGC TAC GA-3' (forward) and 5'-CTG GAC GCA GAG GGC TTT TA-3' (reverse); TNF-α (NM_012675), 5'-CCC AGA CCC TCA CAC TCA GA- 3' (forward), 5'GCC ACT ACT TCA GCA TCT CG -3'(reverse); and GAPDH (NM_017008), 5'-ATG ACT CTA CCC ACG GCA AG-3' (forward), 5'-CTG GAA GAT GGT GAT GGG TT-3' (reverse).

Western blot analysis

Tissue samples were homogenized in RIPA buffer (10 mM Tris-HCl pH 7.5, 120 mM NaCl, 1% NP-40, 1% sodium deoxycholate, and 0.1% SDS) containing a protease inhibitor cocktail (Roche, Indianapolis, Indiana). Protein concentration was determined by DC protein assay (Bio-Rad, Hercules, California). Equal amounts of serum or tissue homogenates were fractionated on SDS-PAGE and transferred to nitrocellulose membrane. The membrane was incubated with antibodies to CIRP (#10209-2-AP; ProteinTech, Chicago, Illinois), GAPDH (#sc-25778; Santa Cruz, Santa Cruz, California), histone (#9715; Cell Signaling, Danvers, Massachusetts), Bax (#sc-526; Santa Cruz), actin (#A5441; Sigma-Aldrich, St. Louis,

Missouri), cathepsin D (#sc-10725; Santa Cruz), or HMGB1 (#ab18256; Abcam, Cambridge, Massachusetts), followed by secondary antibody-horseradish peroxidase conjugate (SouthernBiotech, Birmingham, Alabama) and developed with a chemiluminescence detection kit (GE Healthcare). Band intensities were quantified with densitometry.

Determination of cytokine levels

TNF-α and IL-6 concentrations in serum, tissue homogenates, and culture medium grown with macrophages were measured by ELISA kits from BioSource (Camarillo, California). HMGB1 levels were determined by Western blotting.

Measurements of transaminases and myeloperoxidase activity

Serum concentrations of AST and ALT were determined by assay kits from Pointe Scientific (Canton, Michigan). To determine myeloperoxidase activity, liver tissues were homogenized in 50 mM phosphate buffer (pH 6.0) containing 0.5% hexa-decyl-trimethyl-ammonium bromide. After centrifugation, supernatant was added to the reaction solution (0.2 mg ml^{-1} O-dianisidine dihydrochloride and 0.2 mM H_2O_2 in phosphate buffer) and the time change of optical density at 460 nm was recorded to calculate the activity.

In vitro hypoxia

Hypoxia was produced using a sealed chamber containing 1% O_2, 5% CO_2, and 94% N_2 placed in an incubator at 37 °C. Culture medium was changed to Opti-MEM I medium (Invitrogen) before subjecting to hypoxia. After 20 h incubation in the hypoxic chamber, cells were recovered at normal culture condition for different time periods and collected for further analyses.

Cell fractionation

For isolation of nuclear and cytoplasmic fractions, RAW 264.7 cell pellets were resuspended in buffer containing 10 mM HEPES/KOH pH 7.9, 1.5 mM $MgCl_2$, 10 mM KCl, 0.5 mM dithiothreitol, and a protease inhibitor cocktail on ice for 15 min. After centrifugation, the supernatant was collected as cytoplasmic fraction and the pellet was resuspended in buffer containing 20 mM HEPES/KOH pH 7.9, 25% glycerol, 420 mM NaCl, 1.5 mM $MgCl_2$, 2 mM EDTA, 0.5 mM dithiothreitol, and a protease inhibitor cocktail on ice for 20 min. After centrifugation, the supernatant was collected as nuclear fraction. The isolation of lysosome was performed with a kit as instructed by Thermo Scientific (Waltham, Massachusetts).

Expression of GFP-CIRP fusion protein

The construction of GFP-CIRP expression plasmid is described in the previous study[21]. RAW 264.7 cells were transfected with the plasmid using LipofectAMINE reagent (Invitrogen). Cells were also transfected with a GFP expression plasmid alone as control for the comparison.

Determination of CIRP release in serum and cultured cells

The conditioned medium from normoxic or hypoxic plus reoxygenated RAW 264.7 cells was incubated with 0.02% deoxycholic acid and 10% trichloroacetic acid at 4 °C overnight for protein precipitation, and it was then subjected to Western blotting. Lactate dehydrogenase activity was determined by an assay kit from Pointe Scientific. Serum CIRP concentration was estimated using serial dilutions of purified CIRP as standard on Western blot analysis.

Recombinant proteins

rmHMGB1 was produced as described previously[32]. Recombinant rat TNF-α was obtained from Biosource. Recombinant human (rh) CIRP (Accession #NP_001271; full length) with C-terminal DDK tag was transfected and expressed from human HEK293 cells and obtained from Origene (Rockville, Maryland). rhTLR2 (Accession #NP_003255; Glu21-Leu590) and rhTLR4 (Accession #O00206; Glu24-Lys631) were transfected and expressed from mouse myeloma NS0 cell line. rhMD2 (Accession #BAA78717; Glu17-Asn160) was transformed and expressed from *E. coli*. The rhTLR4/MD2 complex was purified from NS0 cells co-expressed rhTLR4 (Accession #O00206; Glu24-Lys631) and rhMD2 (Accession #Q9Y6Y9; Glu17-Asn160) with His tag at each protein. All rhTLR2, rhTLR4, and rhMD2 were fused with a 10-His tag at their C-terminus and were obtained from R&D Systems (Minneapolis, Minnesota). rhRAGE (Accession #Q15109; Ala23-Ala344) with C-terminal 6-His tag was transfected and expressed from human HEK293 cells and obtained from Biovision (Milpitas, California).

Synthesis of oligopeptides

A panel (total of 32) of 15-mer oligopeptides with 5 amino acids offsets across the entire human CIRP sequence was synthesized at Genscript (Piscataway, New Jersey). All Fmoc-protected amino acids, solvents, TBTU and 2-chlorotrityl (Cl-Trt) resin were purchased from Sigma-Aldrich. The synthesis of oligopeptide was carried out using Fmoc/tBu solid-phase peptide synthesis (SPPS) strategy on a Tetras automated peptide synthesizer (Creosalus, Louisville, Kentucky). The SPPS protocol consisted of two consecutive deprotection steps and a coupling step. The synthesis was performed on 2-Cl-Trt resin. The crude peptide was precipitated, washed and lyophilized. The purification of the crude peptide was performed by semi-preparative reversed phase high-performance liquid chromatography (RP-HPLC). The peptide was identified by electrospray ionization mass spectrometry (ESI-MS) analysis.

Surface plasmon resonance (SPR) analysis

Analysis of protein-protein and peptide-protein interactions was conducted using the BIAcore T200 instrument (GE Healthcare). Binding reactions were performed in 1× PBS buffer containing 0.01% Tween-20 (pH 7.4). The CM5 dextran chip (flow cell-2) was first activated by injection with 89 μl of 0.1 M N-ethyl-N'-[3-diethylamino-propyl]-carbodiimide and 0.1 M N-hydroxysuccinimide. An aliquot of 200 μl of 5 μg ml^{-1} of the ligand diluted in 10 mM sodium acetate (pH 4.5) was injected into flow cell-2 of the CM5 chip for immobilization. Next, 135 μl of 1 M ethanolamine (pH 8.2) was then injected to block the

remaining active sites. The flow cell-1 without coating with the ligand was used as a control to evaluate nonspecific binding. The binding analyses were performed at flow rate of 30 μl min^{-1} at 25 °C. To evaluate the binding, the analyte (ranging from 62.5 nM to 1.0 μM for kinetics analysis or 0.5 μM for yes or no binding analysis) was injected into flow cell-1 and -2 and the association of analyte and ligand was recorded respectively by surface plasmon resonance. The signal from the blank channel (flow cell-1) was subtracted from the channel (flow-cell 2) coated with the ligand. Data were analyzed by the BIAcore T200 Evaluation Software. For all samples, a blank injection with buffer alone was subtracted from the resulting reaction surface data. Data were globally fitted to the Lagmuir model for a 1:1 binding.

Statistical analysis

Numerical data are expressed as mean ± s.e.m. and compared by one-way analysis of variance (ANOVA) and Student-Newman-Keuls test. Student's *t*-test was used for two-group analysis. Majority of data sets passed the normality test. Some data sets had a statistical difference in the variation between the groups. The survival rate is estimated by the Kaplan-Meier method and compared using the log-rank test. Differences in values were considered significant if $P < 0.05$.

Construction of CIRP expression plasmid

Rat CIRP cDNA (NM_031147) was synthesized from total RNA isolated from rat heart by using MLV reverse transcriptase with oligo $d(T_{16})$ primers. The cDNA was amplified with oligonucleotide primers, sense 5'-CAC CAT GGC ATC AGA TGA AGG-3' and antisense 5'-CTC GTT GTG TGT AGC ATA GC-3'. The resulting PCR product was digested with *Eco*RV and *Not*I and cloned into pENTR vector (Invitrogen) at the C-terminus of hexahistidine tag (His-tag) and then transformed to *E. coli* BL21 (DE3). Individual clones were selected by kanamycin resistance.

Purification of rmCIRP

Transformed *E. coli* carrying rat His-CIRP expression plasmid were inoculated in Luria-Bertani medium containing kanamycin overnight and induced with 1.0 mM IPTG for another 6 h. The bacteria were harvested by centrifugation and the pellet was washed once with 20 mM Tris-HCl pH 7.9. Bacterial pallet was resuspended in buffer containing 20 mM Tris-HCl pH 7.9, 500 mM NaCl, and 5 mM imidazole, and lysed by sonication at 4 °C. The soluble extract was clarified by centrifugation at 20,000*g* at 4 °C for 1 h. The clear lysate was loaded onto a Ni^{2+}-NTA column (Novagen, Madison, Wisconsin). The bound protein was washed with 20 mM Tris-HCl pH 7.9, 500 mM NaCl, and 100 mM imidazole, and was eluted in the same buffer supplemented with 1.0 M imidazole. All proteins were dialyzed with PBS and stored at –80 °C for further analysis.

Removal of LPS from the purified rmCIRP preparation

Triton X-114 (Sigma-Aldrich) was added to the purified protein solution to a final concentration of 5%. The mixture was rotated at room temperature for 15 min to ensure a homogenous solution. Then, the mixture was centrifuged at 14,000*g* for 12 min. The upper

aqueous phase containing rmCIRP (LPS free) was carefully removed. The level of LPS in the removed solution was measured by Limulus amebocyte lysate (LAL) assay (Cambrex, East Rutherford, New Jersey).

Validation of the purified rmCIRP

The purity of rmCIRP preparation was examined by SDS-PAGE staining with Coomassie blue, showing a major band at 24 kDa and very minor bands at other positions (**Supplementary Fig. 3a**). The identity of rmCIRP was further confirmed by Western blotting against antibodies to CIRP from two different sources, one generated from our laboratory and the other from ProteinTech (**Supplementary Fig. 3b**). The purified rmCIRP was further validated by amino acid sequence analysis using LC-MS/MS at the Proteomics Resource Center of the Rockefeller University, New York. The recombinant protein was identified as CIRP with >95% confidence using the MASCOT database search algorithm.

Production of antisera to CIRP

Antisera against the purified rmCIRP were raised in New Zealand White rabbits by standard procedures at Covance (Princeton, New Jersey). The IgG fraction was isolated from antisera by immobilized immunopure protein-A and -G chromatography (Pierce). The specificity of antisera to CIRP was examined by Western blotting against its purified protein. LPS was undetectable in the antiserum preparations as measured by LAL assay (Cambrex). The same process was performed to purify rabbit serum control IgG.

Supplementary Material

Refer to Web version on PubMed Central for supplementary material.

ACKNOWLEDGEMENTS

This work was supported by US National Institutes of Health (NIH) grants HL076179 and GM053008 (P.W.). We thank H. Erlandsson-Harris (Karolinska Institute, Stockholm, Sweden) for providing *Rage*$^{-/-}$, *Tlr2*$^{-/-}$, and *Tlr4*$^{-/-}$ mice, M. Hu, J.H. Li, and L.M. Corbo for technical assistance, L. Caracappa for editorial assistance, and Y. Al-Abed and A. Ragab for the assistance with SPR analysis. BIAcore instrument was supported by NIH S10OD012042. J.F. was partly supported by the Smoking Research Foundation of Japan.

REFERENCES

1. Holcomb JB, et al. Challenges to effective research in acute trauma resuscitation: consent and endpoints. Shock. 2011; 35:107–113. [PubMed: 20926987]
2. Bulger EM, et al. Hypertonic resuscitation of hypovolemic shock after blunt trauma: a randomized controlled trial. Arch. Surg. 2008; 143:139–148. [PubMed: 18283138]
3. Kaczorowski DJ, Mollen KP, Edmonds R, Billiar TR. Early events in the recognition of danger signals after tissue injury. J. Leukoc. Biol. 2008; 83:546–552. [PubMed: 18032691]
4. Dombrovskiy VY, Martin AA, Sunderram J, Paz HL. Rapid increase in hospitalization and mortality rates for severe sepsis in the United States: a trend analysis from 1993 to 2003. Crit. Care Med. 2007; 35:1244–1250. [PubMed: 17414736]
5. Ward PA. New approaches to the study of sepsis. EMBO Mol. Med. 2012; 4:1234–1243. [PubMed: 23208733]
6. Medzhitov R. Origin and physiological roles of inflammation. Nature. 2008; 454:428–435. [PubMed: 18650913]

7. Oppenheim JJ, Yang D. Alarmins: chemotactic activators of immune responses. Curr. Opin. Immunol. 2005; 17:359–365. [PubMed: 15955682]
8. Zhang X, Mosser DM. Macrophage activation by endogenous danger signals. J. Pathol. 2008; 214:161–178. [PubMed: 18161744]
9. Beutler BA. TLRs and innate immunity. Blood. 2009; 113:1399–1407. [PubMed: 18757776]
10. Ward PA. The sepsis seesaw: seeking a heart salve. Nat. Med. 2009; 15:497–498.
11. Kawai T, Akira S. The role of pattern-recognition receptors in innate immunity: update on Toll-like receptors. Nat. Immunol. 2010; 11:373–384. [PubMed: 20404851]
12. Chen GY, Tang J, Zheng P, Liu Y. CD24 and Siglec-10 selectively repress tissue damage-induced immune responses. Science. 2009; 323:1722–1725. [PubMed: 19264983]
13. Wang H, et al. HMG-1 as a late mediator of endotoxin lethality in mice. Science. 1999; 285:248–251. [PubMed: 10398600]
14. Tsung A, et al. The nuclear factor HMGB1 mediates hepatic injury after murine liver ischemia-reperfusion. J. Exp. Med. 2005; 201:1135–1143. [PubMed: 15795240]
15. Quintana FJ, Cohen IR. Heat shock proteins as endogenous adjuvants in sterile and septic inflammation. J. Immunol. 2005; 175:2777–2782. [PubMed: 16116161]
16. Martinon F, Pétrilli V, Mayor A, Tardivel A, Tschopp J. Gout-associated uric acid crystals activate the NALP3 inflammasome. Nature. 2006; 440:237–241. [PubMed: 16407889]
17. Vogl T, et al. Mrp8 and Mrp14 are endogenous activators of Toll-like receptor 4, promoting lethal, endotoxin-induced shock. Nat. Med. 2007; 13:1042–1049. [PubMed: 17767165]
18. Xu J, et al. Extracellular histones are major mediators of death in sepsis. Nat. Med. 2009; 15:1318–1321. [PubMed: 19855397]
19. Zhang Q, et al. Circulating mitochondrial DAMPs cause inflammatory responses to injury. Nature. 2010; 464:104–107. [PubMed: 20203610]
20. Nishiyama H, et al. Cloning and characterization of human CIRP (cold-inducible RNA-binding protein) cDNA and chromosomal assignment of the gene. Gene. 1997; 204:115–120. [PubMed: 9434172]
21. Nishiyama H, et al. A glycine-rich RNA-binding protein mediating cold-inducible suppression of mammalian cell growth. J. Cell Biol. 1997; 137:899–908. [PubMed: 9151692]
22. Xue JH, et al. Effects of ischemia and H_2O_2 on the cold stress protein CIRP expression in rat neuronal cells. Free Radic. Biol. Med. 1999; 27:1238–1244. [PubMed: 10641716]
23. Nishiyama H, et al. Decreased expression of cold-inducible RNA-binding protein (CIRP) in male germ cells at elevated temperature. Am. J. Pathol. 1998; 152:289–296. [PubMed: 9422546]
24. Nishiyama H, et al. Diurnal change of the cold-inducible RNA-binding protein (Cirp) expression in mouse brain. Biochem. Biophys. Res. Commun. 1998; 245:534–538. [PubMed: 9571190]
25. Sheikh MS, et al. Identification of several human homologs of hamster DNA damage-inducible transcripts. Cloning and characterization of a novel UV-inducible cDNA that codes for a putative RNA-binding protein. J. Biol. Chem. 1997; 272:26720–26726. [PubMed: 9334257]
26. Wellmann S, et al. Oxygen-regulated expression of the RNA-binding proteins RBM3 and CIRP by a HIF-1-independent mechanism. J. Cell Sci. 2004; 117:1785–1794. [PubMed: 15075239]
27. Qu Y, Dubyak GR. P2X7 receptors regulate multiple types of membrane trafficking responses and non-classical secretion pathways. Purinergic Signal. 2009; 5:163–173. [PubMed: 19189228]
28. Aida Y, Pabst MJ. Removal of endotoxin from protein solutions by phase separation using Triton X-114. J. Immunol. Methods. 1990; 132:191–195. [PubMed: 2170533]
29. Wang Y, et al. Identification of stimulating and inhibitory epitopes within the heat shock protein 70 molecule that modulate cytokine production and maturation of dendritic cells. J. Immunol. 2005; 174:3306–3316. [PubMed: 15749862]
30. Henderson B, et al. Caught with their PAMPs down? The extracellular signalling actions of molecular chaperones are not due to microbial contaminants. Cell Stress Chaperones. 2010; 15:123–141. [PubMed: 19731087]
31. Andersson U, et al. High mobility group 1 protein (HMG-1) stimulates proinflammatory cytokine synthesis in human monocytes. J. Exp. Med. 2000; 192:565–570. [PubMed: 10952726]

32. Yang H, et al. Reversing established sepsis with antagonists of endogenous high-mobility group box 1. Proc. Natl. Acad. Sci. USA. 2004; 101:296–301. [PubMed: 14695889]
33. Yang S, Zhou M, Chaudry IH, Wang P. Novel approach to prevent the transition from the hyperdynamic phase to the hypodynamic phase of sepsis: role of adrenomedullin and adrenomedullin binding protein-1. Ann. Surg. 2002; 236:625–633. [PubMed: 12409669]
34. Nagai Y, et al. Essential role of MD-2 in LPS responsiveness and TLR4 distribution. Nat. Immunol. 2002; 3:667–672. [PubMed: 12055629]
35. Hyakushima N, et al. Interaction of soluble form of recombinant extracellular TLR4 domain with MD-2 enables lipopolysaccharide binding and attenuates TLR4-mediated signaling. J. Immunol. 2004; 173:6949–6954. [PubMed: 15557191]
36. Yang C, Carrier F. The UV-inducible RNA-binding protein A18 (A18 hnRNP) plays a protective role in the genotoxic stress response. J. Biol. Chem. 2001; 276:47277–47284. [PubMed: 11574538]
37. Cammas A, Lewis SM, Vagner S, Holcik M. Post-transcriptional control of gene expression through subcellular relocalization of mRNA binding proteins. Biochem. Pharmacol. 2008; 76:1395–1403. [PubMed: 18582437]
38. De Leeuw F, et al. The cold-inducible RNA-binding protein migrates from the nucleus to cytoplasmic stress granules by a methylation-dependent mechanism and acts as a translational repressor. Exp. Cell Res. 2007; 313:4130–4144. [PubMed: 17967451]
39. Yang R, et al. Functional significance for a heterogenous ribonucleoprotein A18 signature RNA motif in the 3'-untranslated region of ataxia telangiectasia mutated and Rad3-related (ATR) transcript. J. Biol. Chem. 2010; 285:8887–8893. [PubMed: 20103595]
40. Qu Y, Franchi L, Nunez G, Dubyak GR. Nonclassical IL-1 beta secretion stimulated by P2X7 receptors is dependent on inflammasome activation and correlated with exosome release in murine macrophages. J. Immunol. 2007; 179:1913–1925. [PubMed: 17641058]
41. Benhamou Y, et al. Toll-like receptors 4 contribute to endothelial injury and inflammation in hemorrhagic shock in mice. Crit. Care Med. 2009; 37:1724–1728. [PubMed: 19325486]
42. Wittebole X, Castanares-Zapatero D, Laterre PF. Toll-like receptor 4 modulation as a strategy to treat sepsis. Mediators Inflamm. 2010; 2010:568396. [PubMed: 20396414]
43. Park JS, et al. Involvement of toll-like receptors 2 and 4 in cellular activation by high mobility group box 1 protein. J. Biol. Chem. 2004; 279:7370–7377. [PubMed: 14660645]
44. Ohashi K, Burkart V, Flohé S, Kolb H. Cutting edge: heat shock protein 60 is a putative endogenous ligand of the toll-like receptor-4 complex. J. Immunol. 2000; 164:558–561. [PubMed: 10623794]
45. Termeer C, et al. Oligosaccharides of Hyaluronan activate dendritic cells via toll-like receptor 4. J. Exp. Med. 2002; 195:99–111. [PubMed: 11781369]
46. Okamura Y, et al. The extra domain A of fibronectin activates Toll-like receptor 4. J. Biol. Chem. 2001; 276:10229–10233. [PubMed: 11150311]
47. Yang H, et al. A critical cysteine is required for HMGB1 binding to Toll-like receptor 4 and activation of macrophage cytokine release. Proc. Natl. Acad. Sci. USA. 2010; 107:11942–11947. [PubMed: 20547845]
48. Yang H, Antoine DJ, Andersson U, Tracey KJ. The many faces of HMGB1: molecular structure-functional activity in inflammation, apoptosis, and chemotaxis. J. Leukoc. Biol. 2013; 93:865–873. [PubMed: 23446148]
49. Shin HJ, et al. Kinetics of binding of LPS to recombinant CD14, TLR4, and MD-2 proteins. Mol. Cell. 2007; 24:119–124.
50. Scaffidi P, Misteli T, Bianchi ME. Release of chromatin protein HMGB1 by necrotic cells triggers inflammation. Nature. 2002; 418:191–195. [PubMed: 12110890]
51. Brochu C, et al. NF-kappaB-Dependent Role for Cold-Inducible RNA Binding Protein in Regulating Interleukin 1beta. PLoS One. 2013; 8:e57426. [PubMed: 23437386]
52. Sakurai T, et al. Cirp protects against tumor necrosis factor-alpha-induced apoptosis via activation of extracellular signal-regulated kinase. Biochim. Biophys. Acta. 2006; 1763:290–295. [PubMed: 16569452]

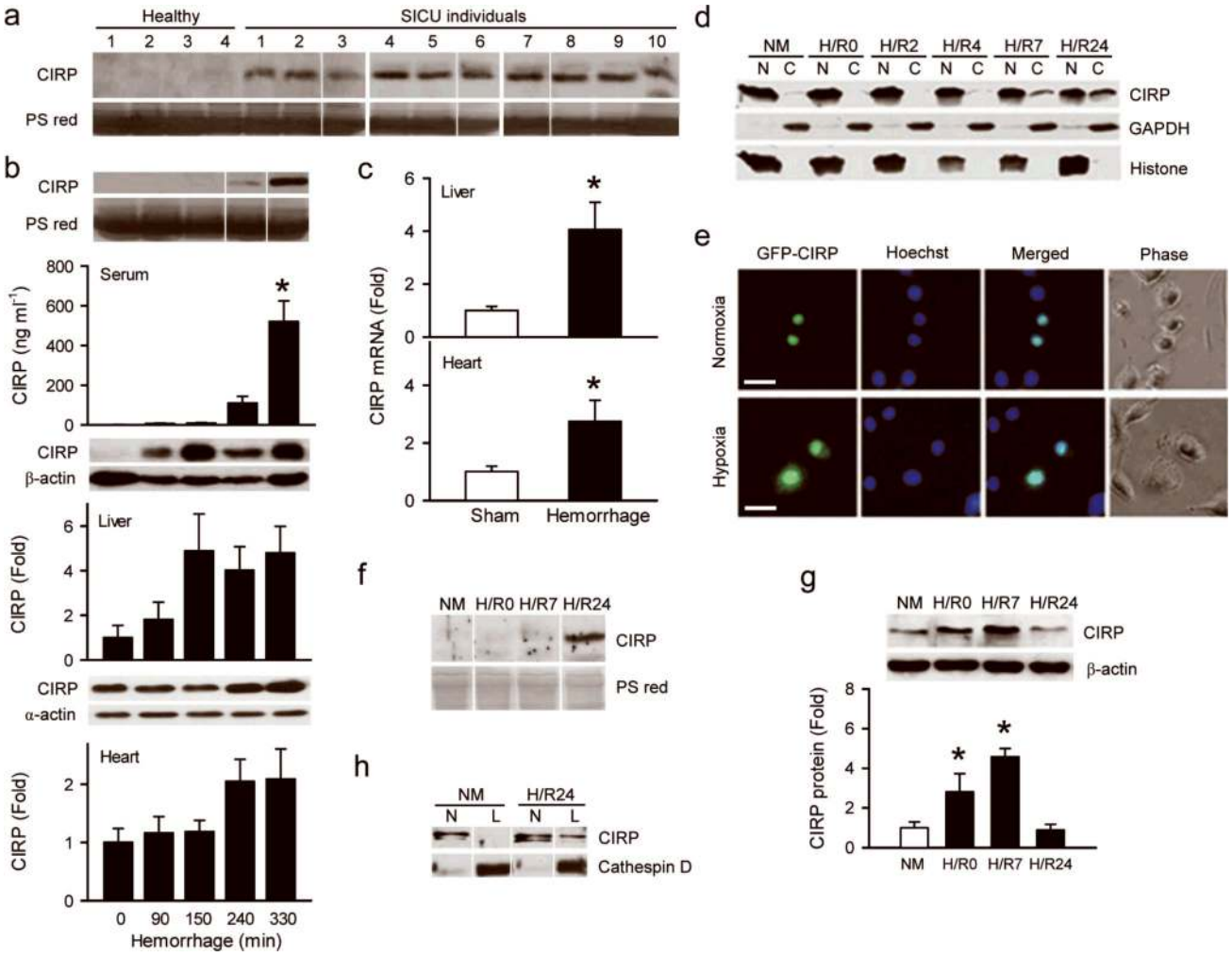

Figure 1.

Expression and release of CIRP after hemorrhage. (**a**) Western blot analysis of CIRP in the serum of healthy volunteers and surgical intense care unit (SICU) individuals with shock. (**b**) Western blot analysis of CIRP in the tissues of rats at the indicated times post-hemorrhage. $n = 4–6$ per time-point, $^*P < 0.05$ *vs*. time 0, determined by one way ANOVA and Student-Newman-Keuls test. (**c**) qPCR analysis of CIRP mRNA in the liver and heart of rats at 240 min post-hemorrhage. $n = 6$ per group, $^*P < 0.05$ *vs*. sham, determined by Student's *t*-test. (**d**) Western blot analysis of CIRP in the nuclear (N) and cytoplasmic (C) components of RAW 264.7 cells cultured in normoxia (NM) or exposed to hypoxia (1% O_2) for 20 h, followed by reoxygenation for 0, 2, 4, 7, or 24 h (H/R0, H/R2, H/R4, H/R7, or H/R24). Antibody to GAPDH and histone for detecting the cytoplasm and nucleus, respectively. (**e**) Images of RAW 264.7 cells expressing GFP-CIRP (green) and Hoechst 33245 (blue) staining of nuclei. Scale bar, 25 μm. (**f**) Western blot analysis of CIRP in the conditioned medium or (**g**) total cell lysate from RAW 264.7 cells. $n = 3$ per group, $^*P < 0.05$ *vs*. NM, determined by one way ANOVA and Student-Newman-Keuls test. (**h**) Western blot analysis of CIRP in the nuclear (N) and lysosomal (L) components of RAW 264.7 cells cultured in normoxia or exposed to hypoxia (H/24R). Antibody to cathepsin D

for detecting the lysosomes. Images represent three independent experiments (**d–h**). Data are mean ± s.e.m. (**b,c,g**). PS red, Ponceau S red staining. For Western blot images, small gap indicates skip lanes from the same membrane; large gap indicates separate membranes.

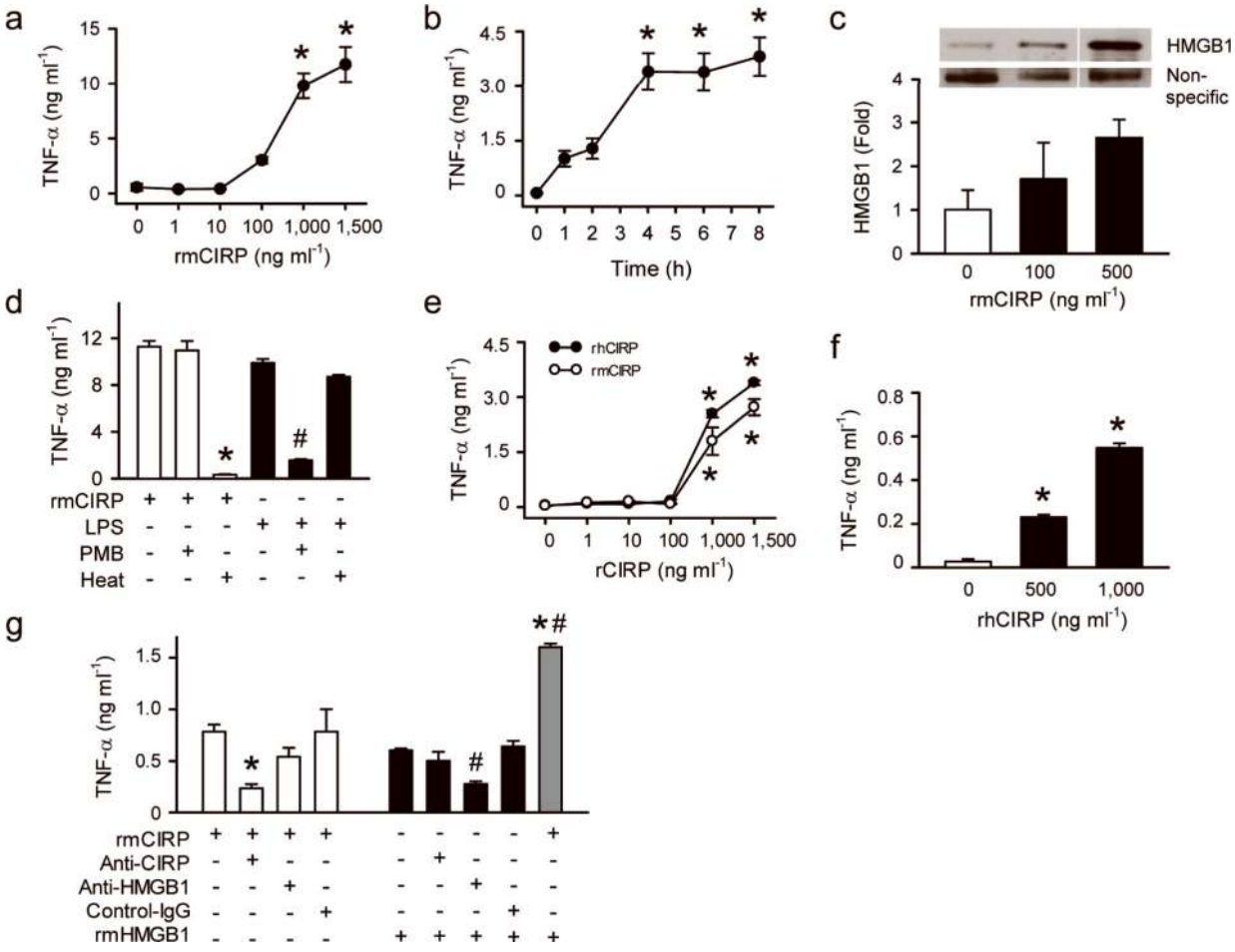

Figure 2.

Recombinant CIRP induces cytokine release in macrophages. (**a,b**) TNF-α production of RAW 264.7 cells stimulated with various concentrations of rmCIRP for 4 h or rmCIRP (100 ng ml^{-1}) for various time periods. *P < 0.05 *vs*. no rmCIRP or time 0. (**c**) Western blot analysis of HMGB1 in the conditioned medium from RAW 264.7 cells stimulated with various concentrations of rmCIRP for 20 h. For the images, small gap indicates skip lanes from the same membrane. (**d**) TNF-α production of RAW 264.7 cells stimulated with rmCIRP (1.5 μg ml^{-1}) or LPS (10 ng ml^{-1}) for 8 h with (+) or without (–) polymyxin B (PMB; 120 U ml^{-1}) and heat (at 80 °C for 30 min). *P < 0.05 *vs*. rmCIRP; $^{\#}P$ < 0.05 *vs*. LPS. (**e**) TNF-α production of differentiated human THP-1 cells stimulated with rhCIRP or rmCIRP at various concentrations for 4 h. *P < 0.05 *vs*. no CIRP. (**f**) TNF-α production of human PBMC stimulated with various concentrations of rhCIRP for 8 h. *P < 0.05 *vs*. no rhCIRP. (**g**) TNF-α production of THP-1 cells stimulated with rmCIRP (0.3 μg ml^{-1}), rmHMGB1 (0.3 μg ml^{-1}), or rmCIRP plus rmHMGB1 for 8 h, with (+) or without (–) 1 h pre-incubation of antisera to CIRP (Anti-CIRP; 4 μg ml^{-1}), antisera to HMGB1 (Anti-HMGB1; 4 μg ml^{-1}), and rabbit control (non-immunized) IgG (4 μg ml^{-1}). *P < 0.05 *vs*. rmCIRP; $^{\#}P$ < 0.05 *vs*. rmHMGB1. All data are mean ± s.e.m. from three or four independent experiments. Statistical significance was determined by one way ANOVA and Student-Newman-Keuls test.

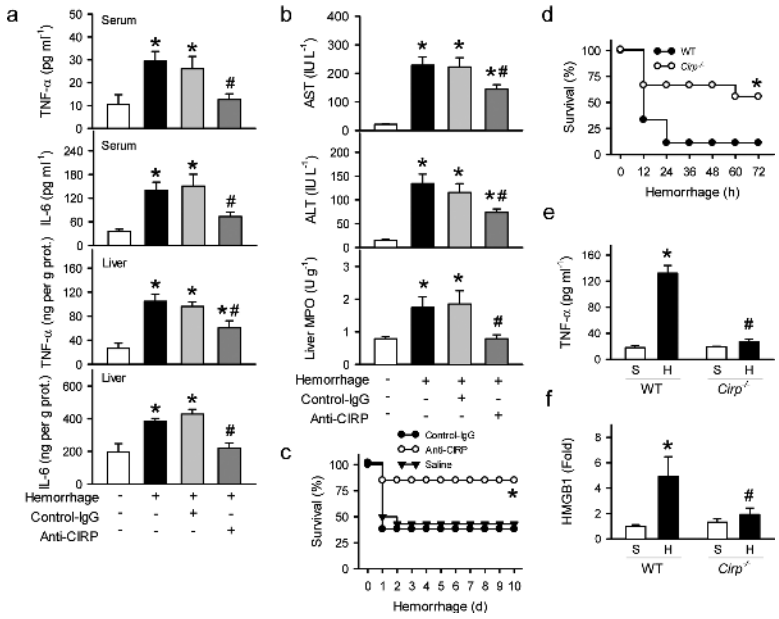

Figure 3.

Attenuation of cytokine production and hepatic injury by antisera to CIRP after hemorrhage. (**a,b**) The levels of TNF-α and IL-6 in the serum and liver as well as hepatic injury markers AST, ALT, and liver myeloperoxidase (MPO) activity of rats at 4 h post-hemorrhage. Hemorrhaged rats received rabbit control (non-immunized) IgG or antisera to CIRP (Anti-CIRP; 10 mg kg^{-1} body weight) during fluid resuscitation. $n = 6$ per group, $^{*}P < 0.05$ *vs*. sham; $^{\#}P < 0.05$ *vs*. hemorrhage alone. (**c**) Survival curves of hemorrhaged rats administered normal saline (vehicle; $n = 14$), control IgG (10 mg kg^{-1} body weight, $n = 13$), or antisera to CIRP (Anti-CIRP; 10 mg kg^{-1} body weight, $n = 13$) for three consecutive days. $^{*}P < 0.05$ *vs*. saline. (**d**) Survival curves of hemorrhaged wild-type (WT) and *Cirp*$^{-/-}$ mice. $n = 9$ per group, $^{*}P < 0.05$ *vs*. WT. (**e,f**) Serum TNF-α and HMGB1 levels of WT and *Cirp*$^{-/-}$ mice at 4 h post-hemorrhage. $n = 6$ per group, $^{*}P < 0.05$ *vs*. WT sham; $^{\#}P < 0.05$ *vs*. WT hemorrhage. Data are mean ± s.e.m. Statistical significance was determined by one way ANOVA and Student-Newman-Keuls test (**a,b,e,f**). Statistical significance in survival was compared by the log-rank test (**c,d**).

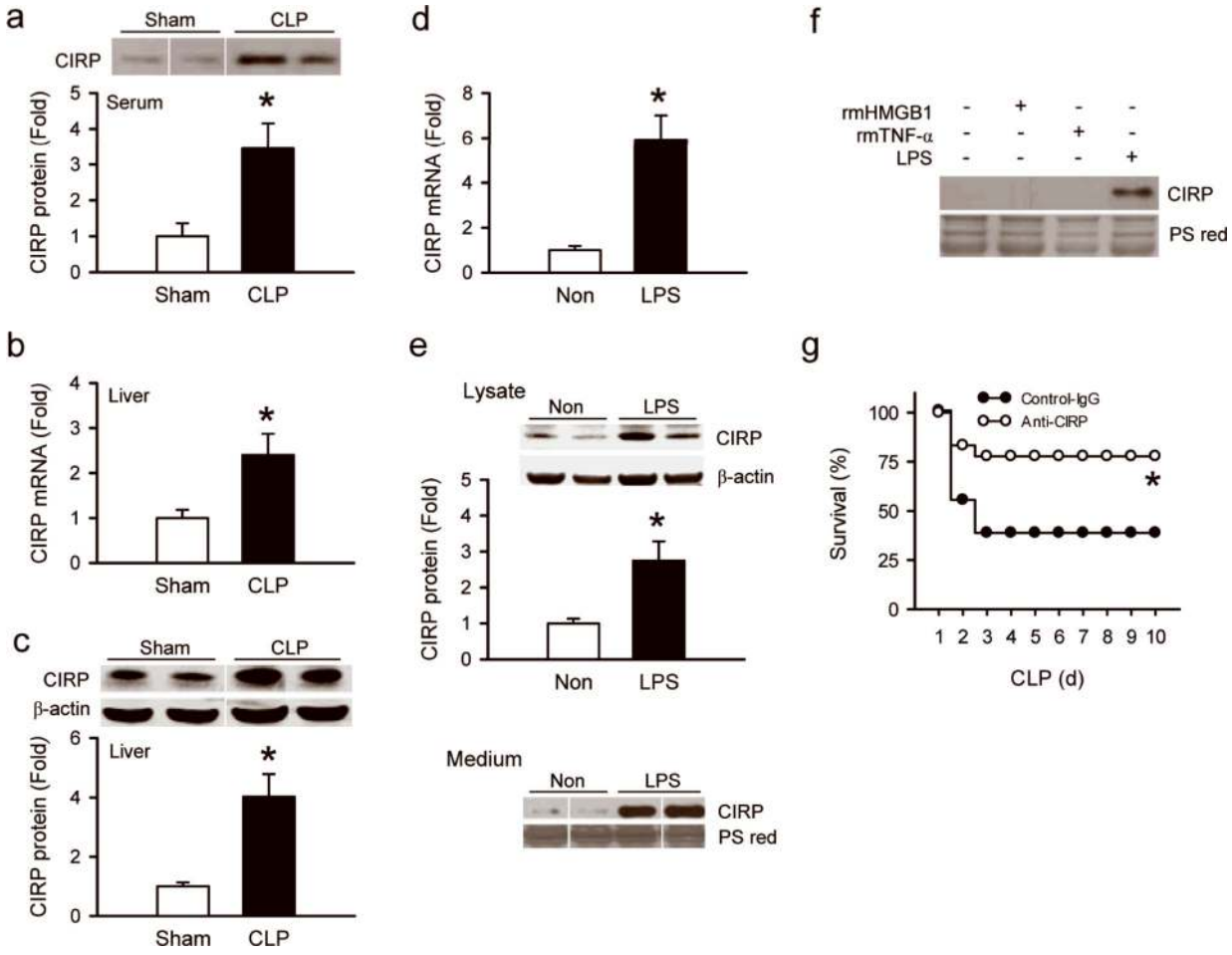

Figure 4.

Expression and release of CIRP after sepsis. (**a–c**) CIRP protein and mRNA expression in the serum and liver of rats at 20 h post-CLP. Data are mean ± s.e.m. $n = 4–6$ per group, $^*P < 0.05$ *vs*. sham, determined by Student's *t*-test. (**d,e**) CIRP mRNA and protein expression in total cell lysate or the conditioned medium from rat peritoneal macrophages either non-treated (Non) or exposed to LPS (10 ng ml^{-1}). CIRP mRNA and protein levels in the conditioned medium were determined after 6 h of LPS exposure. CIRP protein in total cell lysate was determined after 24 h of LPS exposure. Data are mean ± s.e.m. from three independent experiments. $^*P < 0.05$ *vs*. Non, determined by Student's *t*-test. (**f**) Western blot analysis of CIRP in the conditioned medium of RAW 264.7 cells stimulated with (+) or without (–) rmHMGB1 (1 μg ml^{-1}), rmTNF-α (30 ng ml^{-1}) and LPS (100 ng ml^{-1}) for 24 h. Images represent three independent experiments. (**g**) Survival curves of septic rats administered with rabbit control (non-immunized) IgG (10 mg kg^{-1} body weight) or antisera to CIRP (Anti-CIRP; 10 mg kg^{-1} body weight). $n = 18$ per group, $^*P < 0.05$ *vs*. control IgG, determined by the log-rank test. PS red, Ponceau S red staining. For Western blot images, small gap indicates skip lanes from the same membrane.

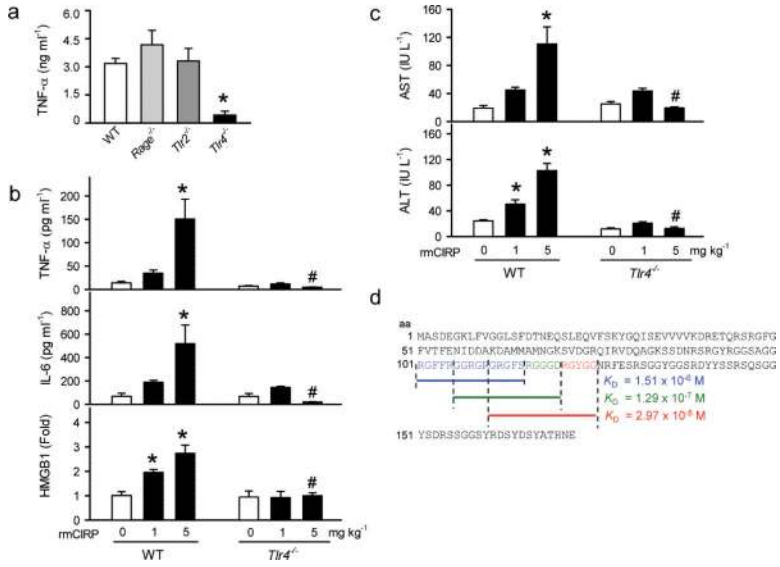

Figure 5.

TLR4/MD2 complex mediates extracellular CIRP activity. (**a**) TNF-α production of peritoneal macrophages from wild-type (WT), *Rage*$^{-/-}$, *Tlr2*$^{-/-}$, or *Tlr4*$^{-/-}$ mice stimulated with rmCIRP (1.5 μg ml^{-1}) for 4 h. Data are mean ± s.e.m. from three independent experiments. *P < 0.05 *vs*. WT. (**b,c**) Serum levels of TNF-α, IL-6, HMGB1, AST, and ALT in WT and *Tlr4*$^{-/-}$ mice at 4 h after administering normal saline (vehicle) or rmCIRP (1 or 5 mg kg^{-1} body weight). Data are mean ± s.e.m. n = 6–9 per group, *P < 0.05 *vs*. WT no rmCIRP; $^{\#}P$ < 0.05 *vs*. WT with rmCIRP (5 mg kg^{-1}). (**d**) Binding affinity (K_D) of three oligopeptides derived from human CIRP sequence to rhMD2. Representative sensorgrams of the oligopeptide analysis are shown in **Supplementary Fig. 6** from two independent experiments. Statistical significance was determined by one way ANOVA and Student-Newman-Keuls test.

Table 1

Binding affinity of rhCIRP to pattern-recognition receptors and MD2

Analyte	Immobilized	K_D (M)
rhCIRP	rhTLR4	6.17×10^{-7}
rhMD2	rhCIRP	3.02×10^{-7}
rhTLR4/MD2	rhCIRP	2.39×10^{-7}
rhMD2	rhTLR4	5.37×10^{-8}
rhRAGE	rhCIRP	3.31×10^{-8}
rhTLR2	rhCIRP	2.58×10^{-7}

Representative sensorgrams of the analyte analysis are shown in **Supplementary Fig. 5** from two to three independent experiments.